Proceeding, 4th Intl. Conf. on Geotechnical Earthquake Engrg and Soil Dynamics, March, 2001, San Diego, CA

LIQUEFACTION ANALYSIS OF LOWER SAN FERNANDO DAM USING STRENGTH RATIOS

Scott M. Olson
University of Illinois-Urbana-Champaign
Urbana, Illinois-USA-61801

Timothy D. Stark
University of Illinois-Urbana-Champaign
Urbana, Illinois-USA-61801

ABSTRACT

Olson (2000) evaluated 33 liquefaction flow failure case histories to assess the yield strength ratio and liquefied strength ratio mobilized during the failures. Using back-analysis procedures developed by Olson (2000), yield and liquefied shear strengths are shown to be proportional to the pre-failure vertical effective stress and are related to standard and cone penetration resistances.

This paper examines the triggering of liquefaction and subsequent flow failure of Lower San Fernando Dam using yield and liquefied strength ratios. The yield strength ratio is used to correctly predict the occurrence of liquefaction in the upstream hydraulic fill of the dam, and the liquefied shear strength ratio is used to correctly predict the subsequent flow failure of the upstream slope. The relationships for the yield and liquefied ratios are presented, and their application to existing or new structures is illustrated using the Lower San Fernando Dam case history.

INTRODUCTION

A liquefaction analysis for ground subjected to a static shear stress, i.e., slopes, embankments, or foundations of structures, typically consists of three tasks: (1) a flow failure susceptibility analysis; (2) a triggering analysis; and (3) a post-triggering/flow failure stability analysis. Existing liquefaction analysis procedures have a number of shortcomings, including a lack of verification using field case histories, the need for expensive and difficult sampling and laboratory testing (Poulos et al. 1985 method), and large correction factors (Seed and Harder 1990 method).

Olson (2000) developed a comprehensive liquefaction analysis procedure that addresses the three tasks and overcomes these shortcomings. Back-analysis of 33 field case histories of statically- and seismically-induced liquefaction flow failure provide the foundation of the analysis procedure. The case histories were back-analyzed to evaluate the shear strength available at the triggering of liquefaction, or the yield shear strength [s_u(yield)], and the shear strength available during flow failure, or the liquefied shear strength [s_u(LIQ)]. Olson (2000) developed back-analyses to determine the yield and liquefied strength ratios directly. The resulting yield and liquefied strength ratios are related to corrected standard and cone penetration resistances to characterize increases in strength ratio with decreasing state parameter (Been and Jefferies 1985).

The proposed liquefaction analysis is illustrated using the Lower San Fernando Dam (LSFD) case history. Firstly, the upstream and downstream hydraulic fill of LSFD is found to be susceptible to liquefaction flow failure, i.e., in a contractive state, using the results of penetration tests conducted in 1985. Secondly, the yield strength ratio is used to correctly predict the occurrence of liquefaction in the upstream hydraulic fill and non-occurrence of liquefaction in the downstream fill. Lastly, the liquefied shear strength ratio is used to correctly predict the subsequent flow failure of the upstream slope.

YIELD AND LIQUEFIED STRENGTH RATIOS AND RELATION TO PENETRATION RESISTANCE

The yield shear strength of a saturated, contractive, sandy soil is defined as the peak shear strength available during undrained loading (Terzaghi et al. 1996). The shear strength mobilized at large deformation is the liquefied shear strength. The yield and liquefied strength ratios are the yield and liquefied shear strengths normalized with respect to the vertical effective stress within the zone of liquefaction prior to failure, respectively. Numerous investigators have shown that the yield and liquefied shear strength of many loose (i.e., contractive), compressible sandy soils are linearly proportional to the effective stress. Olson (2000) details the concepts of the yield and liquefied strength ratios and provides examples of this behavior.

Olson (2000) correlated both the yield strength ratio and liquefied strength ratio to corrected standard penetration test (SPT) blowcount and cone penetration test (CPT) tip resistance. The correlations are reasonable because both the strength ratios and the penetration resistance are functions of soil density and effective confining stress. For example, Been et al. (1987) related normalized CPT tip resistance to state parameter, indicating that higher values of normalized tip resistance correspond to lower values of state parameter. Further, lower values of state parameter correspond to higher values of liquefied strength ratio (e.g., Fear and Robertson 1995). Therefore, higher values of liquefied strength ratio correspond to higher normalized penetration resistance. The same trend should apply for the yield strength ratio.

CASE HISTORY BACK-ANALYSIS RESULTS

Olson (2000) collected and analyzed thirty-three liquefaction flow failures for which SPT and/or CPT results were available or could be reasonably estimated. Olson (2000) describes the available information and references, the development of the back-analyses, the back-analyses conducted, the evaluation of penetration resistance, and the uncertainties and assumptions for each case history.

Yield Strength Ratio

Figure 1 presents the best estimates of yield and mobilized strength ratio and mean corrected SPT and CPT penetration resistance, respectively. Olson (2000) discusses the potential sources of uncertainty for each case history. Despite these uncertainties, and excluding the Nerlerk berm cases (cases 19-21) and seismically-induced failures, a trend of increasing yield strength ratio with increasing penetration resistance is observed in Fig. 1. As discussed by Olson (2000), the deformation- and seismically-induced liquefaction cases are unlikely to provide accurate estimates of yield strength ratio. Only static loading-induced failures provide back-calculated shear strengths and strength ratios that correspond directly to the yield shear strength and strength ratio.

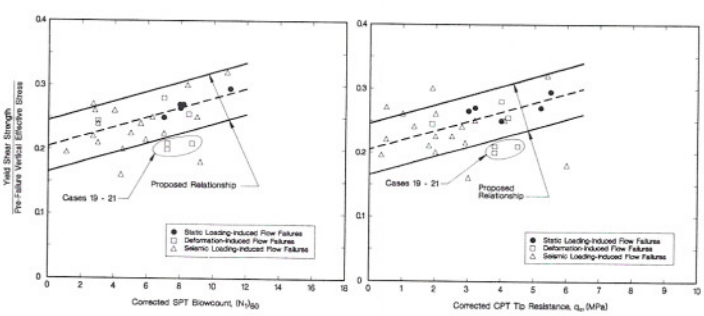

Fig. 1. SPT and CPT based yield strength ratio relationships (from Olson 2000)

Two of the deformation-induced and a few of the seismically-induced flow failures in Fig. 1 plot above the average trend of the static loading-induced failures. Therefore, there may be greater variability in the relationship between yield strength ratio and penetration resistance than that indicated by the five static loading-induced cases. As a result, the upper and lower trendlines were positioned conservatively to account for this variability. The average trendlines proposed are described as:

$$\frac{s_u(yield)}{\sigma'_{vo}} = 0.205 + 0.0075\left[(N_1)_{60}\right] \pm 0.04 \quad (1a)$$

$$\frac{s_u(yield)}{\sigma'_{vo}} = 0.205 + 0.143(q_{c1}) \pm 0.04 \quad (1b)$$

for values of $(N_1)_{60} \leq 12$ and $q_{c1} \leq 6.5$ MPa, respectively.

Liquefied Strength Ratio and Penetration Resistance

Figure 2 presents the best estimates of liquefied strength ratio and mean corrected SPT and CPT penetration resistance, respectively. Olson (2000) discusses the potential uncertainties for each case history. Despite these uncertainties, a reasonable trend in the data is apparent, particularly for the cases where the most information is available (cases plotted with a solid, half-solid, or open circle in Fig. 2). Regression of the trendlines excluded the cases where only the simplified analysis was conducted (cases plotted as triangles in Fig. 2), which are described as:

$$\frac{s_u(LIQ)}{\sigma'_{vo}} = 0.03 + 0.075\left[(N_1)_{60}\right] \pm 0.03 \quad (2a)$$

$$\frac{s_u(LIQ)}{\sigma'_{vo}} = 0.03 + 0.143(q_{c1}) \pm 0.03 \quad (2b)$$

for values of $(N_1)_{60} \leq 12$ and $q_{c1} \leq 6.5$ MPa, respectively. The upper and lower bounds in Fig. 2 approximately correspond to plus and minus one standard deviation.

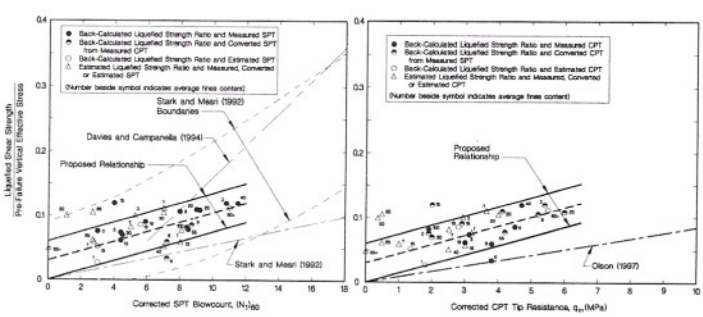

Fig. 2. SPT and CPT based liquefied strength ratio relationships and existing relationships (from Olson 2000)

LIQUEFACTION ANALYSIS OF GROUND SUBJECTED TO A STATIC SHEAR STRESS

Using the yield and liquefied strength ratio correlations shown in Figs. 1 and 2, Olson (2000) proposed a comprehensive

procedure for liquefaction analysis of ground subjected to a static shear stress. This procedure addresses flow failure susceptibility, triggering of liquefaction, and post-triggering stability. In addition, the procedure does not require laboratory testing or large correction factors. The proposed liquefaction analysis procedure is applied to the Lower San Fernando Dam case history to illustrate its ease of use and functionality.

Liquefaction Flow Failure of Lower San Fernando Dam

On February 9, 1971, a massive slide occurred in the upstream (u/s) slope of the Lower San Fernando Dam (LSFD) as a result of the San Fernando earthquake (M ~ 6.6). Seed et al. (1973) conducted an extensive field and laboratory investigation to evaluate the causes of the slide. A pre- and post-failure cross-section of the Lower San Fernando Dam determined by Seed et al. (1973) is shown in Fig. 3. Seed et al. (1973) concluded that seismic shaking triggered liquefaction of the hydraulic fill within the upstream slope of the dam, and seismoscope records indicated that the slide occurred about 30 seconds after the end of shaking (Seed 1979). Only gravitational forces were available to initiate the slope failure. Therefore, it appears that the slide was the result of the loss of strength in the liquefied soils rather than the result of inertia forces during earthquake shaking (Castro et al. 1989; Seed et al. 1989).

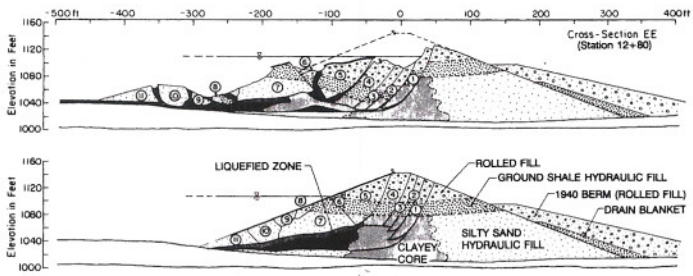

Fig. 3. Cross-section through Lower San Fernando Dam showing: (a) conditions after 1971 earthquake; and (b) schematic reconstruction of failed cross-section (from Castro et al 1992)

Liquefaction Flow Failure Susceptibility

A flow failure susceptibility analysis determines whether a given soil deposit is in a contractive state, i.e., susceptible to undrained strain-softening behavior. Using liquefaction flow failure case histories, Olson (2000) confirmed that the boundary relationship proposed by Fear and Robertson (1995) can be used to delineate conditions susceptible and not susceptible to flow failure using either SPT or CPT penetration resistance.

Figure 4a presents $(N_1)_{60}$ data from the downstream (d/s) slope of LSFD (obtained in the 1985 field investigation). Two boundary relations are shown in the figure, with the solid boundary corresponding to the Fear and Robertson (1995) relation and the dashed boundary augmented to correspond to conditions in the upstream slope of LSFD. The augmented boundary was developed by increasing the $(N_1)_{60}$-axis of the original boundary by 3. This increase accounts for post-earthquake densification [$(N_1)_{60}$ increase of 2] and differing effective stress conditions between the d/s and u/s slopes [$(N_1)_{60}$ increase of 1] as recommended by Seed et al. (1989). Figure 4b presents available q_{c1} data also from the d/s slope of LSFD. The solid line represents the average q_{c1} values and the dashed lines are the minimum and maximum q_{c1} values with depth. Included in Fig. 4b are boundary relations that separate contractive from dilative conditions. The solid boundary relation was converted from the SPT relationship shown in Fig. 4a using $q_c/N_{60} \cong 0.6$ (typical of clean sands). Similar to the SPT relation, the dashed CPT boundary was augmented to correspond to u/s slope conditions by increasing the q_{c1}–axis by 1.2 MPa. The increase was estimated by multiplying the $(N_1)_{60}$ increase of 3 by $q_c/N_{60} \cong 0.4$ (using the median D_{50} from LSFD of approximately 0.12 mm; Stark and Olson 1995).

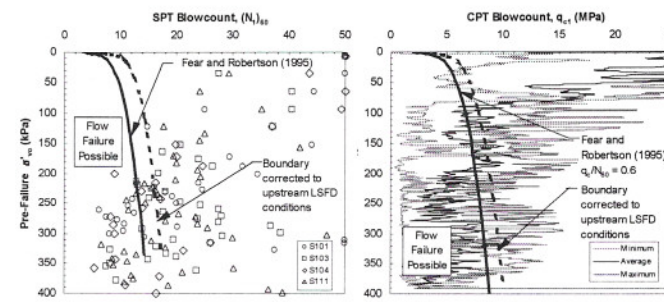

Fig. 4. Comparison of 1985 penetration test results with contractive/dilative boundaries (CPT data from soundings 101, 103, 104, 106, 108, and 109)

Averaging the SPT and CPT results in Fig. 4 suggests that the hydraulic fill in the upstream slope at initial vertical effective stresses (σ'_{vo}) greater than 120 kPa is contractive and therefore susceptible to flow failure. In the downstream slope, hydraulic fill at σ'_{vo} greater than 190 kPa is contractive. The zones of contractive soil are shaded in Fig. 5.

Liquefaction Triggering Analysis

Analysis Procedure. A liquefaction triggering analysis for ground subjected to a static shear stress determines whether the applied shear stresses exceed the yield shear strength of the contractive soil. Olson (2000) proposed the following procedure to conduct a liquefaction triggering analysis.

1. Conduct a slope stability back-analysis of the pre-failure geometry to estimate the static driving shear stress ($\tau_{driving}$) in the contractive (liquefiable) soil(s).
2. Divide the yield failure surface into a number of segments (see Fig. 5). Ten to fifteen segments are satisfactory.
3. Determine the weighted average σ'_{vo} along the yield failure surface and calculate the average static driving shear stress ratio, $\tau_{driving}/\sigma'_{vo}$.

4. Estimate the average seismic shear stress (τ_{ave}) applied to each segment of the failure surface using Eq. (3) (Seed and Idriss 1971) or a site response analysis.

$$\tau_{ave,seismic} = \left(0.65 \frac{a_{max}}{g} \sigma_{vo}(ave) r_d \right) \Big/ C_M \qquad (3)$$

5. If applicable, estimate other shear stresses (τ_{other}) applied to each segment of the yield failure surface using appropriate analyses.

6. Estimate $s_u(yield)/\sigma'_{vo}$ using corrected SPT and/or CPT penetration resistance and Eqs. (1a) and/or (1b). The desired level of conservatism can be incorporated by using a penetration resistance smaller than the mean value, or by selecting a yield strength ratio higher or lower than the mean value.

7. Calculate the values of $s_u(yield)$ and $\tau_{driving}$ *for each segment* of the yield failure surface by multiplying the yield strength and static shear stress ratios by the σ'_{vo} for the segment, respectively.

8. The potential to trigger liquefaction in each segment can then be estimated using a factor of safety against triggering of liquefaction as follows:

$$FS_{Triggering} \approx \frac{s_u(yield)}{\tau_{driving} + \tau_{ave,seismic} + \tau_{other}} \qquad (4)$$

Segments with a $FS_{Triggering}$ greater than unity are unlikely to liquefy. These segments should be assigned their yield shear strength in a post-triggering stability analysis. Segments with a $FS_{Triggering}$ less than or equal to unity are likely to liquefy and the liquefied shear strength should be assigned to these segments for a post-triggering stability analysis. The authors also recommend that several potential failure surfaces be analyzed as the ratio of $\tau_{driving}/\tau_{ave,seismic}$ may vary between failure surfaces.

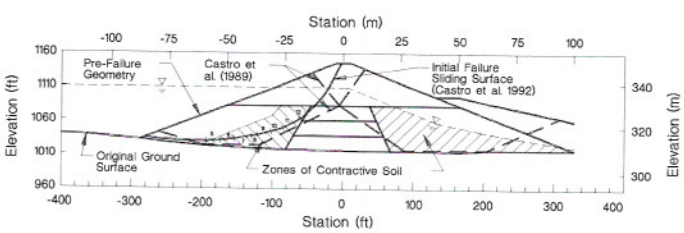

Fig. 5. Pre-failure geometry of LSFD showing zones of contractive soil and potential u/s and d/s yield failure surfaces

LSFD Triggering Analysis. The initial failure surface shown in Fig. 5 (from Castro et al. 1992) resulted in an average static driving shear stress of 31 kPa, with a range of 25 to 36 kPa. This value agrees with values obtained by Seed et al. (1989) and Castro et al. (1989) for slightly deeper failure surfaces. The shear strengths presented in Table 1 (from Castro et al. 1989) were used for the analyses. The yield (initial) failure surface was divided into 16 segments. Of these 16 segments, only segments 5 through 12 are within the zone of liquefiable soil (Fig. 5). Table 2 presents the liquefaction triggering analysis for segments 5 through 12. As indicated in Table 2, the combined static driving and seismic shear stresses trigger liquefaction in segments 5-12. The zone of soil predicted to liquefy by this analysis is nearly identical to that predicted by Seed et al. (1973) and agrees reasonably with the observations by Seed et al. (1989) (see Figs. 3 and 5).

Table 1. Shear Strength Values for Back-Calculations (from Castro et al. 1989)

Layer No.	Soil description	Minimum c (kPa)	Minimum ϕ (°)	Maximum c (kPa)	Maximum ϕ (°)
1	Alluvium	0	40	0	40
2	Starter dikes, non-liquefiable hydraulic fill, rolled fill, and ground shale	0	30	0	35
3	1929-1930 Rock blanket and 1940 Berm	0	40	0	40
4	Upper core	62	0	94	0
5	Middle core	77	0	115	0
6	Lower core	91	0	136	0
7	U/S liquefiable hydraulic fill	b/c[1]	0	b/c	0
8	D/S liquefiable hydraulic fill	b/c	0	b/c	0

[1]b/c = back-calculated value

Other LSFD Triggering Analyses. A number of other triggering analyses were conducted to evaluate the ability of this procedure to predict the performance of LSFD. These analyses, summarized in Table 3 and discussed in a subsequent section, include:

- U/S slope subjected to 1971 San Fernando Eqk. (M~6.6)
- U/S slope subjected to 1952 Kern County Eqk. (M~7.7)
- U/S slope subjected to a hypothetical M~6.6 Eqk. to determine the a_{max} required to cause a flow failure
- U/S slope subjected to a hypothetical M~7.7 Eqk. to determine the a_{max} required to cause a flow failure
- U/S slope subjected to 1971 San Fernando Eqk. using the failure surface suggested by Castro et al. (1989)
- U/S slope subjected to a hypothetical M~6.6 Eqk. to determine the a_{max} required to cause a flow failure along the failure surface suggested by Castro et al. (1989)
- D/S slope subjected to 1971 San Fernando Eqk. using the failure surface suggested by Castro et al. (1989)

Post-Triggering/Flow Failure Stability Analysis

If liquefaction is triggered, a post-triggering stability analysis of the structure (using the pre-failure geometry) must be conducted to determine whether the static driving forces are greater than the available shear resistance. The liquefied shear strength ratio is estimated using Eq. (2). Appropriate values of

Table 2. Summary of Liquefaction Triggering Analysis for the Upstream Slope of the Lower San Fernando Subjected to 1971 San Fernando Earthquake ($M \sim 6.6$, $a_{max} \sim 0.55g$; $C_M \sim 1.39$)

Segment No.	σ'_{vo} (kPa)	σ_{vo} (kPa)	r_d	Ave. s_u(yield) (kPa)	Average $\tau_{driving} / \sigma'_{vo}$	$\tau_{driving}$ (kPa)	$\tau_{ave,seismic}$ (kPa)	$FS_{Triggering}$	Liquefaction Triggered?	Ave. s_u(LIQ) (kPa)
5	120	247	0.82	33.8	0.23	21.8	57.3	0.43	Yes	12.8
6	144	293	0.76	40.6	0.23	26.1	62.6	0.46	Yes	15.4
7	156	322	0.72	43.9	0.23	28.3	65.1	0.47	Yes	16.6
8	168	345	0.69	47.4	0.23	30.5	66.6	0.49	Yes	17.9
9	178	357	0.67	50.1	0.23	32.2	67.1	0.50	Yes	19.0
10	189	374	0.65	53.3	0.23	34.3	67.8	0.52	Yes	20.2
11	207	374	0.65	58.4	0.23	37.6	67.8	0.55	Yes	22.1
12	216	351	0.68	60.7	0.23	39.1	66.9	0.57	Yes	23.0

s_u(LIQ) then are calculated (using the segment values of σ'_{vo}) and assigned to the segments of the failure surface predicted to liquefy. Fully mobilized drained or undrained shear strengths are assigned to the non-liquefied soils. This analysis should be conducted for all of the potential failure surfaces that were examined in the triggering analysis.

If the factor of safety against flow failure, FS_{Flow}, is less than or equal to unity, flow failure is predicted to occur. However, if the FS_{Flow} is between unity and about 1.1, some deformation probably will occur. If this is the case, segments of the failure surface with marginal $FS_{Triggering}$ (approximately 1.0 to 1.1) should be reassigned the liquefied shear strength. This accounts for the potential for deformation-induced liquefaction and progressive failure of the entire structure. The post-triggering stability analysis then should be repeated until there is no significant decrease in the FS_{Flow}.

The results of the post-triggering stability analyses conducted for both the u/s and d/s slopes of LSFD under a variety of triggering conditions also are summarized in Table 3.

Discussion of Results

As indicated in Table 3, the proposed liquefaction analysis procedure predicts that liquefaction was triggered in the upstream slope during the 1971 San Fernando earthquake. The resulting FS_{Flow} was approximately 0.85, correctly predicting that a flow failure would occur. The same conclusion was reached using the Castro et al. (1989) u/s failure surface, with FS_{Flow} of approximately 0.72. For comparison, Castro et al. (1989) calculated $FS_{Flow} = 0.54$ and Seed et al. (1973, 1989) calculated $FS_{Flow} = 0.80$ when s_u(LIQ) was assumed to be zero.

Table 3. Summary of Liquefaction Triggering and Flow Failure Stability Analyses

Slope	Earthquake	M_L	Actual a_{max} (g)	a_{max} req'd to cause cause flow failure (g)	Segments triggered to liquefy	Average FS against flow failure	FS range[1]
U/S	1971 San Fernando	6.6	0.5 (min)	--	5 - 12 (all)	0.85	0.77 - 0.92
			0.6 (max)	--	5 - 12 (all)		
U/S	1952 Kern County	7.7	0.05 (min)	--	none	1.23	1.15 - 1.30
			0.12 (max)	--	5 - 9	1.01	0.94 - 1.08
U/S	Hypothetical	6.6	--	0.17	5 - 9	1.01	0.94 - 1.08
U/S	Hypothetical	7.7	--	0.12	5 - 9	1.01	0.94 - 1.08
U/S	1971 San Fernando using	6.6	0.5 (min)	--	2 - 10 (all)	0.72	0.64 - 0.79
	Castro et al. failure surface		0.6 (max)	--	2 - 10 (all)		
U/S	Hypothetical using	6.6	--	0.09	2 - 6	0.95	0.87 - 1.02
	Castro et al. failure surface						
D/S	1971 San Fernando using	6.6	0.5 (min)	--	none	1.72	1.63 - 1.80
	Castro et al. failure surface		0.6 (max)	--	3, 9, 10	1.55	1.46 - 1.63

[1]FS range reports values obtained using lower and upper bound shear strengths in the non-liquefied soils and core

The 1952 Kern County earthquake (M~7.7) was the largest earthquake that LSFD was subjected to prior to 1971. Castro et al. (1989) indicated that the 1952 earthquake likely caused peak surface accelerations on the order of 0.05 to 0.12g. Seed et al. (1989) reported that slightly elevated porewater pressures were measured in the foundation soils below the downstream rolled fill buttress two days after the earthquake. Because the u/s hydraulic fill was looser than the soil within and below the d/s fill, it should have experienced a larger porewater pressure increase, but this does not necessarily imply that liquefaction was triggered.

These observations agree with the performance of the upstream slope predicted by the proposed procedure. The procedure indicates that no liquefaction would be triggered under the minimum acceleration (0.05g), with $FS_{Triggering}$ of approximately 1.2 to 1.3. Under the maximum acceleration (0.12g), segments 5 to 9 (see Fig. 5) liquefy marginally, with a $FS_{Triggering}$ of approximately 0.9 to 1.0. The resulting FS_{Flow} averaged 1.23 and 1.01 for the respective accelerations.

Castro et al. (1989) suggested that LSFD could have withstood a M ~ 6.6 earthquake that produced accelerations of 0.12 to 0.15g without causing a flow failure. Seed et al. (1989) suggested that LSFD could have withstood slightly larger accelerations of 0.13 to 0.30g. The proposed liquefaction analysis procedure indicates that LSFD could have withstood similar accelerations, from approximately 0.09 to 0.17g during a M 6.6 and about 0.12g during a M 7.7 earthquake without causing a flow failure.

Finally, Castro et al. (1989) suggested that the downstream slope had a FS_{Flow} of approximately 1.0 prior to the upstream slide. Seed et al. (1989) reported that minor excess porewater pressures were measured below the downstream slope following the 1971 earthquake, in agreement with analytical results from Seed et al. (1973). The predicted performance of the downstream slope agreed well with the observed performance. The calculations indicated that only minor liquefaction was possible, but not likely, during the 1971 earthquake, and the FS_{Flow} for the d/s slope (prior to the u/s slide) was approximately 1.55 to 1.72.

CONCLUSIONS

Olson (2000) proposed a comprehensive liquefaction analysis procedure for ground subjected to a static shear stress to overcome shortcomings in existing methods. The procedure uses yield and liquefied strength ratios back-calculated from liquefaction flow failure case histories, and addresses: (1) flow failure susceptibility; (2) liquefaction triggering; and (3) a post-triggering/flow failure stability analysis.

The proposed liquefaction analysis procedure was verified using the Lower San Fernando Dam case history. The proposed procedure accurately predicted the performance of both the upstream and downstream slope when subjected to the 1971 San Fernando and the largest previous earthquakes. Firstly, the procedure predicted liquefaction and flow failure of the upstream slope during the 1971 earthquake, while predicting only minor to no liquefaction in the downstream slope. Secondly, the analysis predicted satisfactory performance of the upstream slope during the 1952 Kern County earthquake, the largest previous earthquake to which the dam was subjected. Lastly, parametric studies indicated that the dam could likely have withstood shaking on the order of 0.09 to 0.17g without causing a flow failure. This result agrees with results from Castro et al. (1989) (a_{max} ~ 0.12-0.15g) and Seed et al. (1989) (a_{max} ~ 0.13-0.3g).

REFERENCES

Been, K. and M.G. Jefferies [1985]. A state parameter for sands. *Geotechnique*, 35(2), 99-112.

Been, K., M.G. Jefferies, J.H.A. Crooks, and L. Rothenburg [1987] The cone penetration test in sands: part II, general inference of state. *Geotechnique*, 37(3), 285-299.

Castro, G., T.O. Keller, and S.S. Boynton [1989]. Re-evaluation of the Lower San Fernando Dam: Report 1, an investigation of the February 9, 1971 slide. *U.S. Army Corps of Engineers Contract Report GL-89-2*, Volumes 1 and 2, U.S. Army Corps of Engineers Waterways Experiment Station, Vicksburg, Mississippi.

Castro, G., R.B. Seed, T.O. Keller, and H.B. Seed [1992]. Steady-state strength analysis of Lower San Fernando Dam slide. *ASCE J. of Geot. Eng.*, 118(3), 406-427.

Fear, C.E. and P.K. Robertson [1995]. Estimating the undrained strength of sand: a theoretical framework. *Canadian Geot. J.*, 32(4), 859-870.

Olson, S.M. [2000]. Liquefaction resistance and the shear strength of liquefied soil from penetration resistance. *Mid-America Earthquake Center Report*, in press, to be available at http://mae.ce.uiuc.edu.

Poulos, S.J., G. Castro. and W. France [1985]. Liquefaction evaluation procedure. *ASCE J. of Geot. Eng. Div.*, 111(6), 772-792.

Seed, H.B. [1979]. Considerations in the earthquake-resistant design of earth and rockfill dams. *Geotechnique*, 29(3), 215-263.

Seed, H.B. and I.M. Idriss [1971]. Simplified procedure for evaluating soil liquefaction potential. *ASCE J. of Geot. Eng. Div.*, 97(SM9), 1249-1273.

Seed, H.B., K.L. Lee, I.M. Idriss, and F. Makdisi [1973]. Analysis of the slides in the San Fernando Dams during the earthquake of Feb. 9, 1971. *Earthquake Engineering Research Center 73-2*, University of California, Berkeley, Calif.

Seed, H.B., R.B. Seed, L.F. Harder, and H.-L. Jong [1989]. Re-evaluation of the Lower San Fernando Dam: Report 2, examination of the post-earthquake slide of February 9, 1971. *U.S. Army Corps of Engineers Contract Report GL-89-2*, U.S. Army Corps of Engineers Waterways Experiment Station, Vicksburg, Mississippi.

Seed, R.B. and L.F. Harder [1990]. SPT-based analysis of cyclic pore pressure generation and undrained residual strength. *Proc., H.B. Seed Memorial Symp.*, Bi-Tech Publishing Ltd., Vol. 2, 351-376.

Stark, T.D. and S.M. Olson [1995]. Liquefaction resistance using CPT and field case histories. *ASCE J. of Geot. Eng.*, 121(12), 856-869.

Terzaghi, K., R.B. Peck, and G. Mesri [1996]. *Soil Mechanics in Engineering Practice, Third Edition*. John Wiley & Sons, Inc., New York.